Solid Freeform Fabrication 2017: Proceedings of the 28th Annual International Solid Freeform Fabrication Symposium – An Additive Manufacturing Conference
Reviewed Paper

Fabrication and characterization of Graphite/Nylon 12 composite via binder Jetting additive manufacturing process

Hadi Miyanaji[1], Junaid Muhammad Akbar[2], Li Yang[1]

[1]Department of Industrial Engineering, University of Louisville

[2]Department of Mechanical Engineering, University of Louisville

Abstract

Nowadays, graphite is used in many applications due to its unique combination of physical properties. Fabrication of graphite parts has been mostly restricted to traditional manufacturing processes (e.g. moldering), and limited works have been devoted to the feasibility of additive manufacturing (AM) technology to produce graphite components. In the present study, the feasibility of binder jetting additive manufacturing (BJ-AM) process in fabrication of graphite/nylon composites is investigated. The printability of the composite parts with varying graphite amount was experimentally examined through the adjustment of in-process parameters (e.g. saturation level and drying energy) and post-processing curing (e.g. curing time and temperature). The efficiency of nylon as the liquid phase sintering agent was studied via the mechanical property evaluation of the composites. In addition, the electrical properties of the graphite/nylon composites were investigated in order to evaluate the effectiveness of the manufacturing method for graphite-based structures for potential functional applications.

Keywords: Binder Jetting Process, Saturation, Composite, Liquid phase sintering

1. Introduction

Additive Manufacturing (AM) technology is referred to as a collection of processes which creates a part geometry through adding materials layer by layer from a digital CAD file. AM allows for highly complex parts to be made while wasting little to no material. One of the popular AM processes is the binder jetting additive manufacturing (BJ-AM) process. BJ-AM utilizes liquid binder to selectively join powder from powder feedstock in order to create 3D geometries. For the fabrication of each layer, after a layer of powder material is spread on top of the powder bed, a printhead selectively deposits certain amount of binder droplets at designated locations of the powder bed. After binder deposition, the entire powder bed surface is subjected to external heating applied via a radiation heat source in order to partially cure the binder and ensure adequate

mechanical strength for subsequent printing processes. After the drying/curing, a new layer of powder will be added to the powder bed, and the process repeats until the entire geometry is printed [1]. Upon completion of the printing process in order to increase the mechanical properties and structural integrity of the green parts, the fabricated parts are further heated in an oven commonly for few hours at temperatures about 200 °C. After curing in the oven, the green parts possess only limited strength and often require additional post-processing such as sintering and infiltration in order to achieve desired mechanical strength [2-4]. Due to the use of binder for geometry creation, BJ-AM technique possesses various advantages over other AM processes, such as the elimination of thermally induced defects (e.g. distortion, unwanted grain growth, etc.) and broad compatibility with exotic materials such as ceramics and refractory metals [2, 5-8].

Graphite is a commonly used material in many industries such as chemical industry, nuclear industry, manufacturing industry, etc. It is also a good candidate for refractory materials (e.g. crucibles, ladles, and molds for containing molten metals) due to its high temperature stability and chemical inertness. Graphite is part of the carbon family and has several desired traits and interesting properties. Most applications utilize unique characteristics of graphite, such as thermal resistance and electrical conductivity or thermal conductivity, self-lubrication, etc. combined with other functional materials as composite structures [9]. The commonly used method for fabrication of graphite/polymer components is the molding of the papered graphite/polymer mixture to produce the desired geometries. There exist different mixing techniques for manufacturing polymer/graphite composites including in situ polymerization, solution compounding and melt blending [10, 11]. In in-situ polymerization method, the monomer is polymerized in the presence of the graphite and as a result, the in-situ compounding technique offers stronger interactions between the graphite and the polymeric phase. In solution compounding, the polymer is dissolved in a solvent and graphite is dispersed in the resulting solution. In the melt bending technique, traditional mixing equipment such as extruder, internal mixer, and two-roll mill can be adopted for the blending operations and are usually available in most compounding units. Some of the restrictions of these processes includes high cost of mixture preparation, high cost of mold fabrication, part design limitations, etc.

The desired properties of graphite coupled with complex geometries that cab be realized by means of the BJ-AM could potentially benefit many industrial applications such as in electronics, computers, casting, electrodes and electrical contacts, etc. One of the challenges in fabrication of

graphite components using the AM process is the transformation of graphite from solid phase to gaseous phase which might take place during sintering of the green parts at high temperatures and under atmospheric pressure [12]. As a result, traditional sintering methods are not suitable to be employed for the post-processing the graphite green parts. In this study, in order to overcome this issue, nylon-12 polymer powder was added to the graphite powder in varying volumetric percentages in the attempt to enable liquid phase sintering in the printed components during post-processing. The added polymer powder is expected to melt and distribute through the graphite matrix under the capillary effects, and consequently increase the mechanical strength of the parts after sintering. The effectiveness of nylon powder as the liquid phase sintering agent is experimentally investigated in terms of mechanical strength (compressive strength) of the printed samples. In addition, the electrical characteristics of the graphite/nylon composites are studied in order to evaluate the effectiveness of the binder jetting process for graphite-based structures for potential functional applications.

2. Methodology

Graphite powder provided by Superior Graphite company and nylon-12 powder material from 3D Systems company were used in varying proportions for preparing the graphite/nylon mixtures. Figure 1 shows the morphology of the powder materials used in this study. Although both powders exhibit irregular particle forms, the nylon-12 particles appear to be shaped more spherically with no sharp edges and relatively consistent in size which attribute to good flowability.

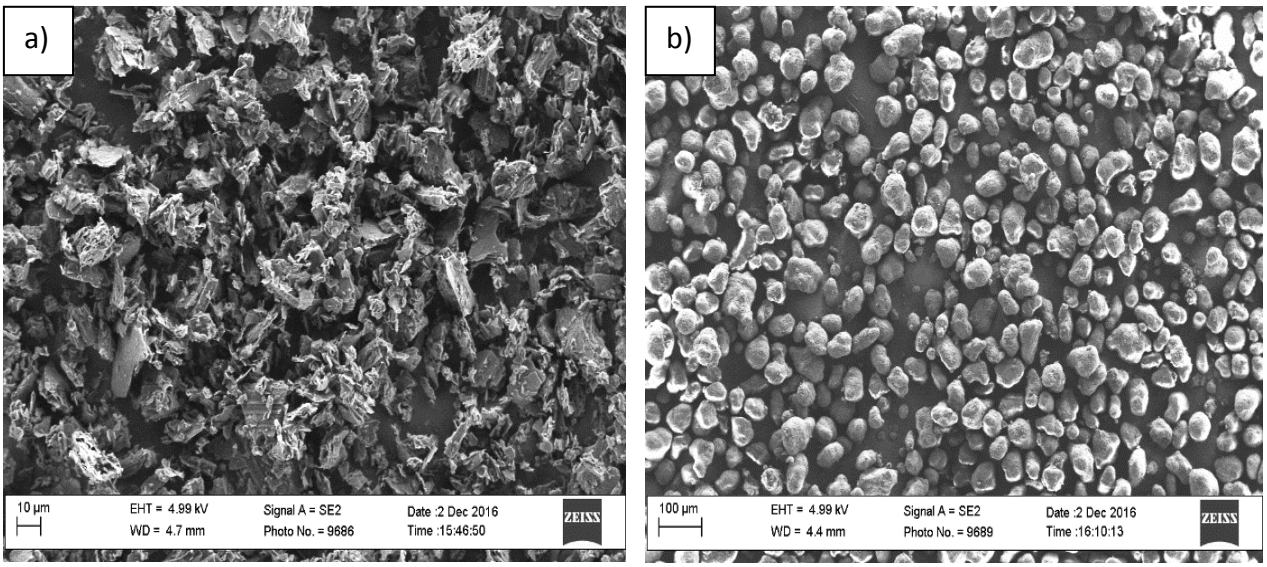

Figure 1. SEM images of a) Graphite powder b) Nylon-12 powder

4 different mixing ratios of graphite to polymer powder were set by volume. The powders were carefully measured and mixed in a clean container before printing. The 4 different ratios of powders used in the study are shown below in Table *1*.

Table 1. Graphite-polymer powder volumetric ratios used for preparing the mixtures

Powder mixture batch	Graphite powder %	Nylon-12 powder %
1	0	100
2	25	75
3	50	50
4	75	25

Ten cubes, each with dimension of 10 mm x 10 mm x 10 mm were printed per batch using the ExOne M-Lab binder jetting printer. In order to achieve the desired mechanical strength of green parts, different saturation levels (the liquid binder amount deposited for each layer of the parts) were examined while the remainder of the process parameters were kept constant during the fabrication process. For all the builds, the in-process binder curing settings (curing power and time) referred to as energy output from the infrared heating lamp used to cure the binding agent during the printing process were set at 75% and 25 seconds for curing power and curing time, respectively, which were determined via preliminary process feasibility studies. Table 2 shows the process parameters used for printing of the parts.

Table 2. Process parameters used for the fabrication

Parameters	Saturation level (%)	Power level (%)	Drying time (s)	Spread speed (mm/s)
Examined level(s)	70, 80, 90	75	25	1.5

The thickness of each powder layer was fixed as 50 micrometers, therefore each of the 10 mm cubes consisted of 200 layers once fully printed. Moreover, through trial and error the powder spreading speed of 1.5 mm/sec was selected which resulted in uniformly spread layers. Figure 2 shows the fabricated green parts before liquid phase sintering process. After fabrication, all the parts were dimensioned using digital calipers (0.01 mm resolution) and weighed using a high resolution digital scale (0.0001g). The compression tests were performed on a Shimadzu micro-tensile testing machine using a 500 N load cell for the green parts and on a Instron 5569A with a

5 KN load cell for the sintered samples. In order to evaluate the electrical properties of the fabricated parts, Fluke 87-5 was used to assess the electrical resistivity of the samples fabricated with varying graphite percentage before and after post-processing. In addition, the microstructure of the sintered samples was analyzed with the aid of ZEISS SUPRATM 35VP SEM equipment to study the effectiveness of liquid phase sintering in the micro scale.

For the liquid phase sintering experiments, parts printed using each of the powder ratios were sintered at 180 °C for 2 hours and at 190 °C for 1 hour in an ExOne electric oven to evaluate the effect of sintering time and temperature on integrity and mechanical strength of the samples. To eliminate variation in sintering, all the samples that needed to be sintered at 180 °C were sintered together in one batch and all the parts that needed to be sintered at 190 °C were sintered together in another batch. The sintering was performed in a SentroTech 6" High Temperature Vacuum Furnace in atmospheric environment.

Figure 2. The printed green parts with different saturation level and various mixtures of graphite/nylon-12

3. Result and discussion

Compression strength of each specimen was calculated using the equation below.

$$\sigma_c = \frac{F_{c,max}}{A_c} \quad (1)$$

where $F_{c,max}$ is the max compression force in Newton and A_c is the cross sectional area of the specimens in meter squared.

The results of compression experimentations for green parts printed with different saturation levels and varying graphite contents are shown in Figure 3. The figure shows that in general as saturation level increases, the compressive strength of the un-sintered parts increases. Such correlation between the saturation amount and the strength of the printed parts has been reported by various researchers for different combinations of binder and powder materials [5, 7, 13, 14]. Higher liquid binder amount in a predefined envelope expands and strengthens the network of the particles connected by the binding agent and as a result, increases the mechanical strength of the printed components. The results also showed that as graphite percentage increases, compressive strength of the green parts exhibits a decreasing trend.

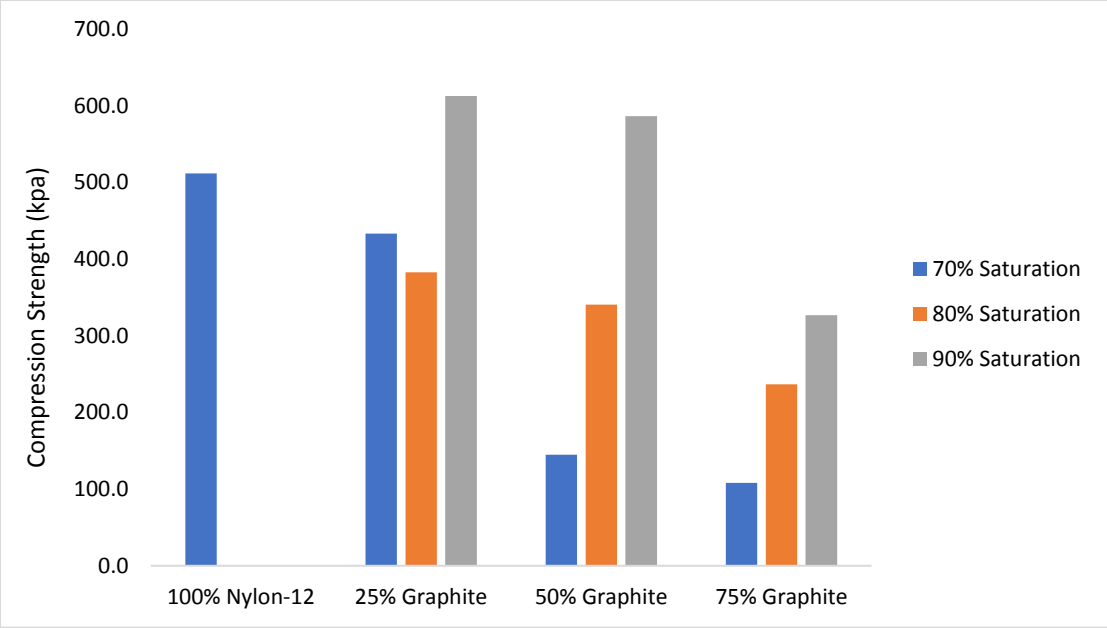

Figure 3. Average compressive strength of green parts

Figure 4 shows the average compressive strength comparison for parts sintered at 180 °C for 2 hours. The figure exhibits similar trends as the un-sintered results from Figure 3. However, the magnitudes of the compressive strength for the sintered parts are greater as expected.

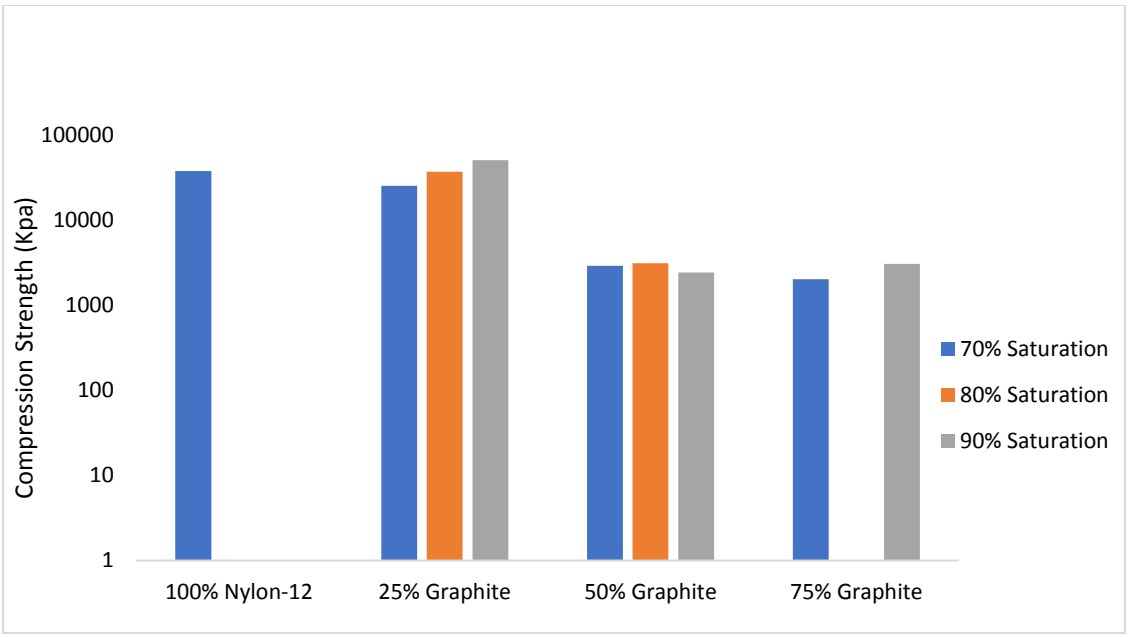

Figure 4. Average compressive strength of the parts sintered at 180 °C for 2 hours

In general, higher saturation leads to higher compressive strength even for the sintered parts in that the higher amount of binding agent in the microstructure of printed samples helps expanding the connection areas between particles and consequently increases the mechanical properties of the parts. For the case of graphite/nylon mixture, since the post-processing temperatures examined (i.e. 180 and 190 °C) are less than the temperature required for the binder burn-out from the microstructure, sintering the parts would not eliminate the binder saturation effect on mechanical characteristics of the fabricated components. At temperatures, higher than the melting point of nylon-12 (i.e. 175 °C), the nylon material melts and disperses through the graphite matrix of the printed parts as the liquid phase sintering agent. The degree of the dispersion and the connectedness of nylon-12 network which largely determines the strength of the sintered components depends not only on the sintering parameters (i.e. temperature and time of sintering) but also on the ratio of materials composing the mixture. With higher magnitude of nylon-12 in the mixture, dispersion of the liquid phase sintering agent in the microstructure becomes more uniform and sufficient as shown in Figure 5. Therefore, such trend of increase in the mechanical properties of the sintering parts is expected as amount of the nylon material in the mixture increases. Figure 6 shows the microstructure of a part sintered at 180 °C for 2 hours with high magnification. The circled region on the figure exhibits a close-up image of graphite/nylon-12 interaction zone with graphite particles surrounded by the molten nylon-12 materials.

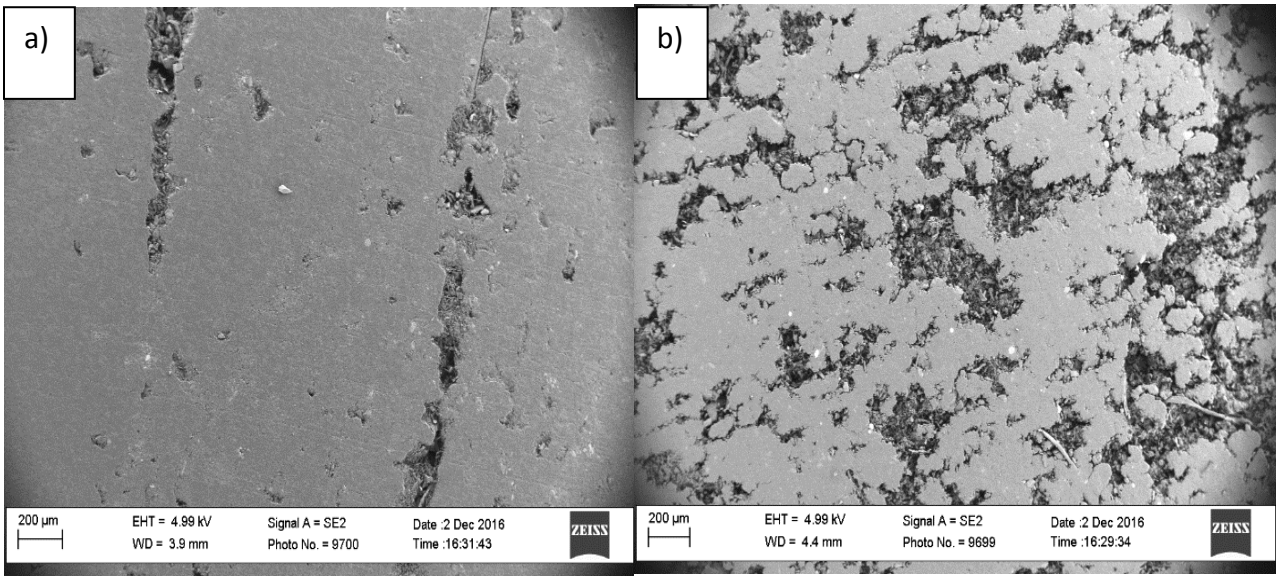

Figure 5. SEM micrographs of specimens containing a) 25% graphite b) 50% graphite

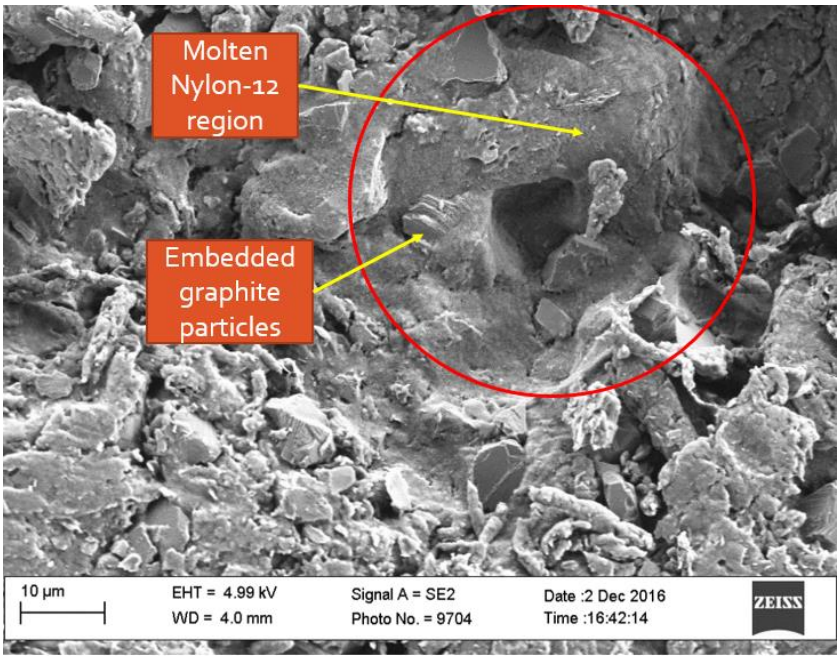

Figure 6. SEM image of a part sintered at 180 °C for 2 hours- Graphite particles surrounded by melted nylon-12

The average compressive strength of the parts processed at 190 °C for 1 hour is shown in Figure 7. Parts sintered at 190 °C for 1 hour exhibit similar compressive strength behavior as previously discussed for other scenarios. The compressive strength increases with higher saturation levels and decreases with higher graphite content.

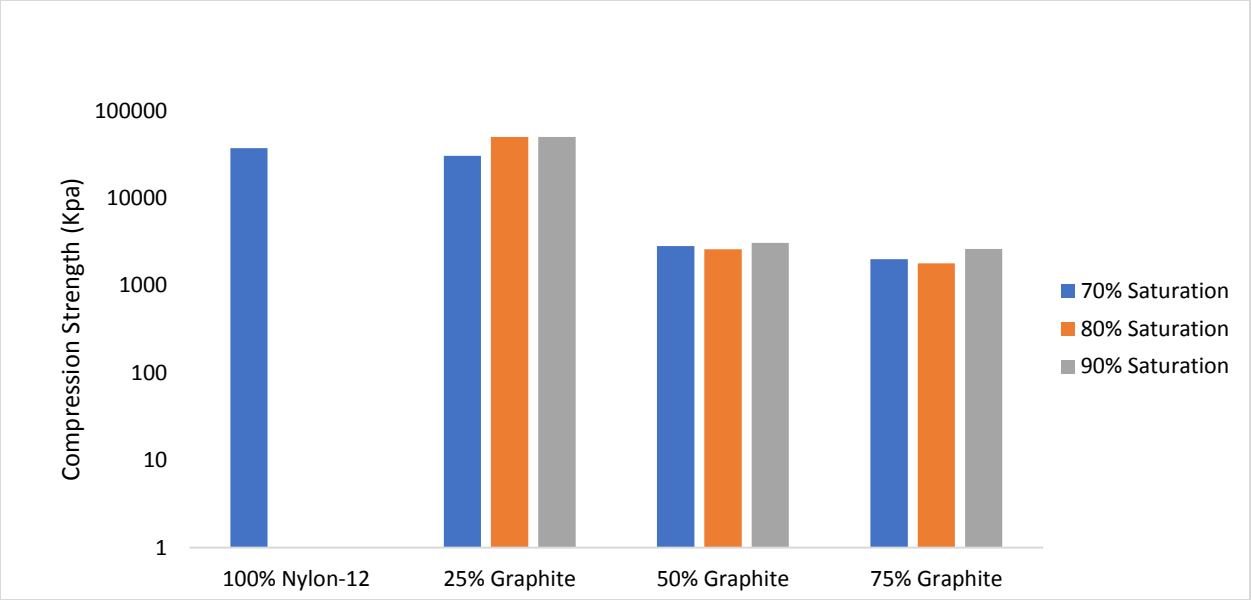

Figure 7. Average compressive strength of the parts sintered at 190 °C for 1 hours

Figure 8 shows direct comparison between the two sintering sets in order to investigate the efficiency of the examined sintering levels. From the figure, it can be concluded the two sintering levels, 180 °C for 2 hours and 190 °C for 1 hour, aren't significantly different and, there isn't an obvious pattern or correlation between sintering levels examined and average compressive strength of parts.

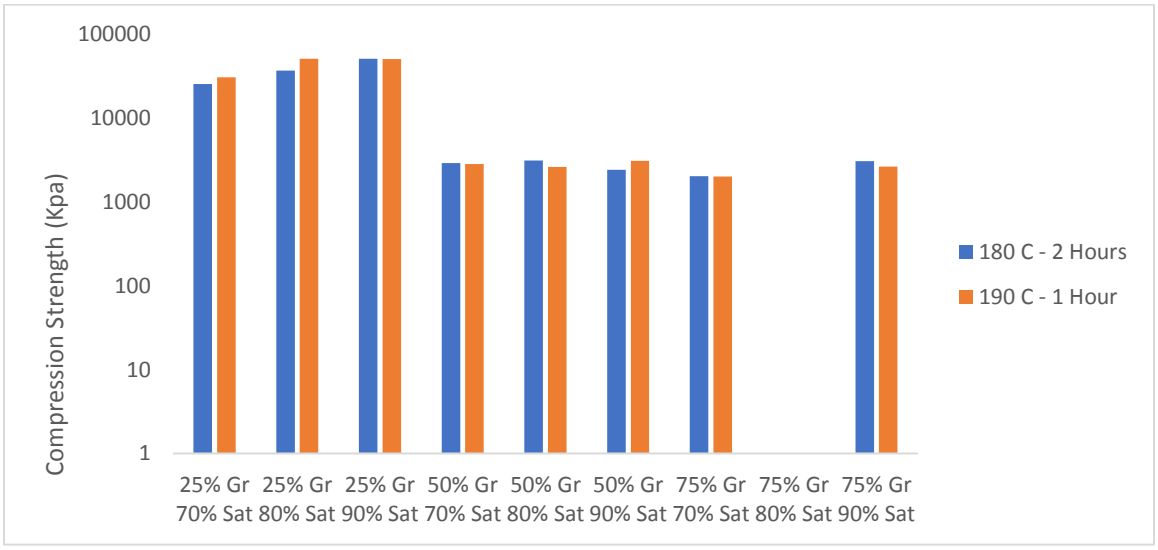

Figure 8. Direct comparison between compressive strength of parts post-processed with both sintering parameters

The electrical resistivity of the parts printed at 90% saturation level before and after sintering performed at 180 °C for 2 hours is shown in Figure 9. Two vertical axes with different scales (KΩ

and Ω) were used for graphing the results due to the significant difference of the sample's electrical resistivity before and after sintering. From the figure, as the graphite magnitude increases in the mixture, the electrical resistivity significantly decreases for both states, before and after sintering. Also, it is observed that the sintering remarkably affects the electrical resistivity of the specimens. Such variation in electrical properties of the samples with post-processing can be partially attributed to the porosity reduction in the microstructure of the samples during sintering in which the molten nylon diffuses through the graphite particles and fill the empty spaces (porosity). Due to the lower electrical resistivity of the nylon-12, 10^{12} Ω, compared to that of air which is approximately 10^{16} Ω, porosity reduction during the post-processing might facilitate the current flow through the microstructure of the printed parts. Another possibility that might explain such effect of post processing is the rearrangement of the graphite particles during sintering due to the forces involved in the interaction between the molten nylon-12 and the particles including the capillary forces.

Figure 10 exhibits the electrical resistivity of the same batch of the samples sintered at 190 °C for 1 hour. The trends observed in the figure are similar to those of parts sintered at 180 °C for 2 hours. It appears that sintering the samples at lower temperatures for longer period of time (at 180 °C for 2 hours) results in slightly better electrical characteristics of the samples likely owing to the more efficient rearrangement of particles during longer sintering time period.

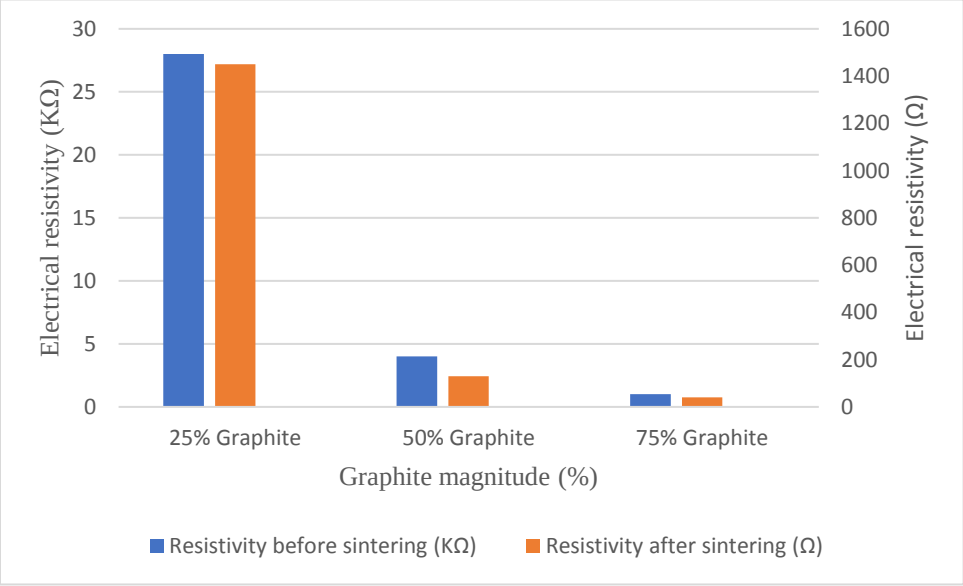

Figure 9. Electrical resistivity of the samples before and after sintering (at 180 °C for 2 hours)

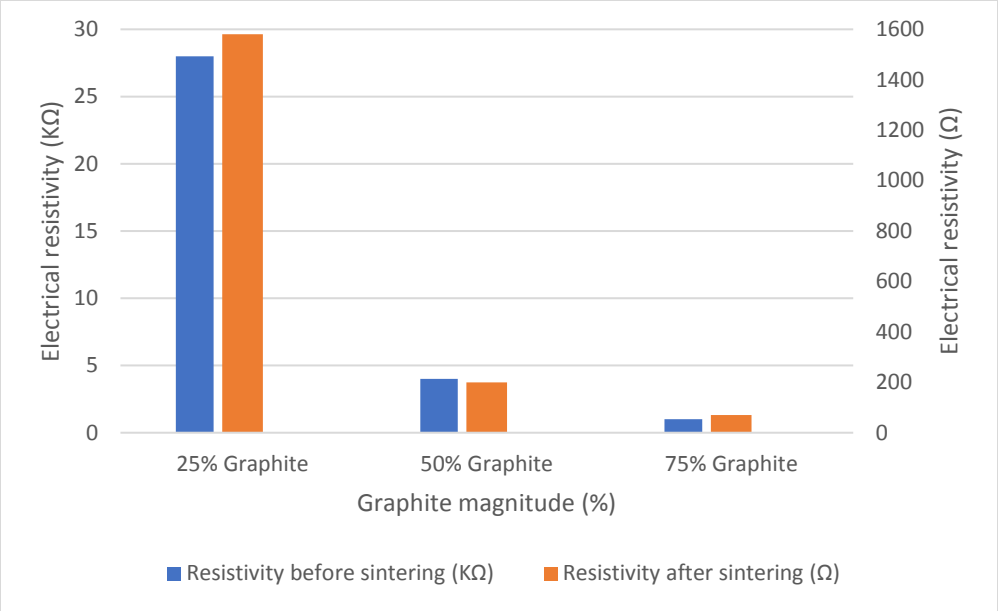

Figure 10. Electrical resistivity of the samples before and after sintering (at 190 °C for 1 hour)

Conclusion

In the present study, the BJ-AM process was applied to fabricate graphite/nylon-12 components. It was shown that the liquid phase sintering process during which nylon-12 melts and disperses through graphite particles was effective in significantly strengthening the printed parts. It was also found that the higher saturation levels generally improved the compressive strength of printed parts. As graphite content increased, the compressive strength of the parts decreased. Within the range of sintering parameters examined, 180 °C for 2 hours and 190 °C for 1 hour, the processed parts performed similarly in terms of mechanical properties. Wider domain of sintering levels could provide more insight into the effect of post-processing parameters on the quality and integrity of the parts fabricated using BJ-AM process. Furthermore, it was shown that the electrical resistivity of the printed samples is significantly influenced by the graphite quantity in the mixture as well as post-processing parameters.

Acknowledgement

The authors are grateful of the material support from Superior Graphite Co. Ltd (Chicago, IL). The authors also want to acknowledge the support from Rapid Prototyping Center (RPC) at University of Louisville.

References

[1] E. Sachs, M. Cima, J. Cornie, Three-Dimensional Printing: Rapid Tooling and Prototypes Directly from a CAD Model, CIRP Annals - Manufacturing Technology 39(1) (1990) 201-204.
[2] J. Moon, A.C. Caballero, L. Hozer, Y.-M. Chiang, M.J. Cima, Fabrication of functionally graded reaction infiltrated SiC–Si composite by three-dimensional printing (3DP™) process, Materials Science and Engineering: A 298(1–2) (2001) 110-119.
[3] B. Utela, D. Storti, R. Anderson, M. Ganter, A review of process development steps for new material systems in three dimensional printing (3DP), Journal of Manufacturing Processes 10(2) (2008) 96-104.
[4] S. Maleksaeedi, H. Eng, F.E. Wiria, T.M.H. Ha, Z. He, Property enhancement of 3D-printed alumina ceramics using vacuum infiltration, Journal of Materials Processing Technology 214(7) (2014) 1301-1306.
[5] J.A. Gonzalez, J. Mireles, Y. Lin, R.B. Wicker, Characterization of ceramic components fabricated using binder jetting additive manufacturing technology, Ceramics International 42(9) (2016) 10559-10564.
[6] J. Yoo, M. Cima, E. Sachs, S. Suresh, Fabrication and Microstructural Control of Advanced Ceramic Components by Three Dimensional Printing, Proceedings of the 19th Annual Conference on Composites, Advanced Ceramics, Materials, and Structures—B: Ceramic Engineering and Science Proceedings, John Wiley & Sons, Inc.2008, pp. 755-762.
[7] S.M. Gaytan, M.A. Cadena, H. Karim, D. Delfin, Y. Lin, D. Espalin, E. MacDonald, R.B. Wicker, Fabrication of barium titanate by binder jetting additive manufacturing technology, Ceramics International 41(5, Part A) (2015) 6610-6619.
[8] A. Winkel, R. Meszaros, S. Reinsch, R. Müller, N. Travitzky, T. Fey, P. Greil, L. Wondraczek, Sintering of 3D-Printed Glass/HAp Composites, Journal of the American Ceramic Society 95(11) (2012) 3387-3393.
[9] C. Research, Graphite (C) - Classifications, Properties and Applications of Graphite. http://www.azom.com/article.aspx?ArticleID=1630, 2002).
[10] B.Z. Jang, A. Zhamu, Processing of nanographene platelets (NGPs) and NGP nanocomposites: a review, Journal of Materials Science 43(15) (2008) 5092-5101.
[11] L. Xie, F. Xu, F. Qiu, H. Lu, Y. Yang, Single-Walled Carbon Nanotubes Functionalized with High Bonding Density of Polymer Layers and Enhanced Mechanical Properties of Composites, Macromolecules 40(9) (2007) 3296-3305.
[12] J.P. Kruth, B. Van der Schueren, J.E. Bonse, B. Morren, Basic Powder Metallurgical Aspects in Selective Metal Powder Sintering, CIRP Annals - Manufacturing Technology 45(1) (1996) 183-186.
[13] M. Vaezi, C.K. Chua, Effects of layer thickness and binder saturation level parameters on 3D printing process, The International Journal of Advanced Manufacturing Technology 53(1) (2011) 275-284.
[14] K. Lu, W.T. Reynolds, 3DP process for fine mesh structure printing, Powder Technology 187(1) (2008) 11-18.